Light-induced atom desorption for cesium loading of a magneto-optical trap: Analysis and experimental investigations

Pengfei Zhang, Gang Li, Yu-chi Zhang, Yanqiang Guo, Junmin Wang, and Tiancai Zhang*
State Key Laboratory of Quantum Optics and Quantum Optics Devices, Institute of Opto-Electronics, Shanxi University, Taiyuan 030006, China
(Received 25 June 2009; published 24 November 2009)

With the help of light-emitting diodes at the center wavelength of 470 nm, we demonstrate that light-induced atom desorption (LIAD) can be used for flexibly controlling the loading of magneto-optical traps (MOT) of cesium atoms. Under an ultralow background pressure in a quartz cell without any wall coating, we show that low intensity blue light can be used to control the loading rates (from 200 to 4000 atoms/s) and the number of cesium atoms (on the order of 10^4 in our experiment) in a MOT without the use of dispensers or any secondary atom source. A theoretical model based on an atom loading rate equation is built which can simulate the magneto-optical trap loading process with LIAD. The theoretical results are in agreement with experimental data. Some important parameters of the vacuum system are determined accordingly. The decay time of the vacuum pressure is about 70 ms, which is much shorter than the usual vacuum system for experiments on atomic ensembles. It is very difficult to measure such short times by the traditional fluorescence detection of cold atoms due to the slow loading process. The change of desorption rate (on the order of 10^{13} atoms/s) for the different desorption intensities is also determined based on the background pressure caused by noncesium atoms in the cell. According to the experimental data and theoretical calculations, we obtain a partial pressure of about 1.4×10^{-10} Torr for the untrapped cesium atoms and about 6.4×10^{-10} Torr for the noncesium atoms at the moment the desorption light is turned off. The system is almost an ideal vacuum system for transferring atoms into another region for further experiments.

DOI: 10.1103/PhysRevA.80.053420 PACS number(s): 37.10.Vz, 68.43.Tj, 68.43.Nr, 37.10.De

I. INTRODUCTION

In the past two to three decades cold atom technology has greatly pushed the development of atomic and molecular physics [1]. Various tools for cooling and trapping atoms have been developed, such as the magneto-optical trap (MOT) [2], magnetic trap [3], optical dipole trap (ODT) [4], optical lattice [5], and so forth. Two research directions have been of intense interest during the last ten years. One is the control of an atomic ensemble for research into atomic coherence, Bose-Einstein condensation (BEC), quantum degenerate Fermi gases, etc. Another is the trapping of a small number of atoms, eventually for deterministic single atom (ion) manipulation, either in a cavity [6] or in free space [7].

However, for all the above-mentioned experiments, the central task is to trap the cold atoms in as robust a way as possible, so the first step is to let the MOT collect the cool atomic cloud in an ultrahigh vacuum. However, a long ensemble lifetime and a large number of atoms are usually incompatible. In a typical experiment that many groups are studying, the microscopic ODT of a single atom in a miniature cavity or free space, it is necessary to increase the number of atoms in the MOT at the beginning to enhance the transfer efficiency of single atoms from the MOT to the ODT. The vacuum becomes poor due to the large number of untrapped atoms in the background, and this decreases the lifetime of the single atoms in the ODT. To resolve this problem, one can use either the atomic beam [7] or double-MOT system [8], but both are usually big and complex. The use of dispensers [9] and light-induced atom desorption (LIAD) [10,11] can essentially overcome this difficulty. A dispenser can release atoms by current heating but the pressure cannot be controlled very efficiently and quickly because of impurities and the relatively slow response of the heating process, respectively. The LIAD process relies on the fact that atoms are adsorbed at the walls of the vacuum chamber and the surfaces of the objects inside the chamber can be desorbed by irradiation of short wavelengths. After shutting off the desorption light the pressure can be restored to equilibrium quickly [12]. This method can solve the above-mentioned problem.

The LIAD effect has been studied for alkali-metal atoms, such as Rb, Na, K, and Cs, but most investigations have focused on wall-coated cells at room-temperature [13–24] and low-temperature cells (1–2 K) [25–27]. It has been used for rubidium MOTs of high loading rates [12,28,29]. In 2006, Klempt *et al.* [12] investigated the loading of cold rubidium atoms in an experimental setup for BEC, and they measured the evolution of the maximum atom number and loading rates with the wavelength and intensity of the desorption light. With relatively high-vacuum pressure they found the decay time of the loading rate was about 200 ms after stopping the desorption process. However, most of the works about LIAD-assisted MOT loading has so far focused on the experimental process and results and its dynamics is not studied in detail. Especially, the influence of LIAD on the background pressure in MOT loading when the desorption process is stopped under a very good vacuum environment, still lack a thorough experimental investigation.

In this paper we report the results of blue light-induced atom desorption in a cesium magneto-optical trap. Our final

*tczhang@sxu.edu.cn

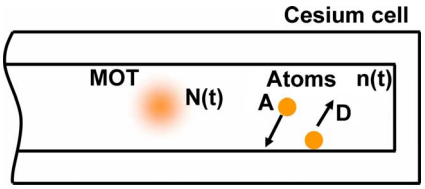

FIG. 1. (Color online) Model of the MOT loading process: two dynamics processes are taken into account: the LIAD process and the MOT loading process. The density of the cesium in the cell $n(t)$ is determined by the absorption coefficient (A) and the desorption rate (D). $1/A$ describes the absorption rate by the surfaces of the glass chamber and other objects inside the chamber; D stands for the atom number desorbed per second. $N(t)$ is the atom number of the MOT.

goal is to trap single cesium atoms with a microscopic dipole trap. Loading the cesium atoms into the MOT from a convenient atomic source is the first step. Detailed analyses of the atomic desorption and reabsorption based on the atomic rate equations allow us to scrutinize these processes, and is corroborated by experiment. We have eventually determined the partial pressure after shutting off the desorption light. The experimental data agree very well with the theory, and the desorption rate D and decay time of the atom density in the cell $(1/A)$ have been obtained. The partial pressure of the untrapped cesium atoms has also been determined. The results reported here may be of value to those groups involved in ultracold atom physics based on cesium.

The paper is organized as follows. In Sec. II we present the theoretical model of atom loading in a magneto-optical trap based on LIAD. The simulation results are shown in Sec. III. In Sec. IV we describe the experimental setup and observation process. The experimental results and the corresponding theoretical analysis are given in Sec. V, and Sec. VI is the conclusion.

II. THEORETICAL MODEL

Let us consider the loading process of a MOT in general with the LIAD process as described in Fig. 1. When the desorption light is turned on, atoms are desorbed from the surfaces of the cell. We use the *desorption rate D* to describe the rate of the desorption, which stands for the atom number desorbed per second. At the same time, atoms in the cell are being adsorbed by the surfaces of the glass chamber and other objects inside the chamber, which is characterized by the *adsorption coefficient A*. $1/A$ describes the adsorption rate. The time evolution of the atom density in the cell can be described by

$$\frac{dn(t)}{dt} = D - An(t). \tag{1}$$

A similar but more complex theoretical model describing the time evolution of the atom density in a coated cell with siloxane film was discussed by Atutov *et al.* in 1999 [15]. Here in our system the cell is not coated and the system works under ultralow background pressure and we have used a simplified model. The atom density is then given by

$$n(t) = \frac{D}{A}(1 - e^{-At}). \tag{2}$$

In principle, when the time approaches infinity, the atom density $n(t)$ reaches the saturation D/A, and if we turn off the desorption light, atoms start to decay and the decay time of $n(t)$ is characterized by $1/A$.

The number of atoms $N(t)$ in the MOT is determined by the following rate Eq. [30]:

$$\frac{dN}{dt} = R - N\left(\frac{1}{\tau_{Cs}} + \frac{1}{\tau_b}\right) - \beta\int n^2 dV. \tag{3}$$

Here R is the loading rate,

$$R = 0.5V^{2/3}v_c^4(m/2kT)^{3/2}n(t). \tag{4}$$

This loading rate depends on the parameters of the MOT, such as the magnetic field, the intensity of the cooling and trapping light and the density of the cesium in the cell $n(t)$. T is the temperature of the environment; m is the mass of cesium atom; V is the trapping volume; v_c is the capture velocity of atoms; and k is Boltzmann's constant. The second term in Eq. (3) represents losses rate due to the collisions between the trapped atoms and the background gas. N/τ_{Cs} is the trap loss rate caused by the collisions of atoms in the MOT with those untrapped background cesium atoms, while N/τ_b stands for the loss rate with the residual noncesium atoms in the background. The last term in Eq. (3) represents the density-dependent losses which can be neglected when the atom number is low in the trap $(\beta=0)$ [31]. The collisions with the untrapped cesium atoms can be expressed [30] as

$$1/\tau_{Cs} = \sigma n(t)(3kT/m)^{1/2}. \tag{5}$$

Here σ is the cross section for an atom to eject a trapped cesium atom.

By using Eqs. (2)–(5), the number of atoms in the MOT can be rewritten as

$$\frac{dN}{dt} = a(1 - e^{-At}) - Nb(1 - e^{-At}) - Nc, \tag{6}$$

where a, b, and c are given by

$$a = 0.5V^{2/3}v_c^4(m/2kT)^{3/2}\frac{D}{A}, \tag{7.1}$$

$$b = \sigma\sqrt{\frac{3kT}{m}}\frac{D}{A}, \tag{7.2}$$

$$c = \frac{1}{\tau_b}. \tag{7.3}$$

The time evolution of the atom number can then be obtained by solving Eq. (6) directly, and we get the general result

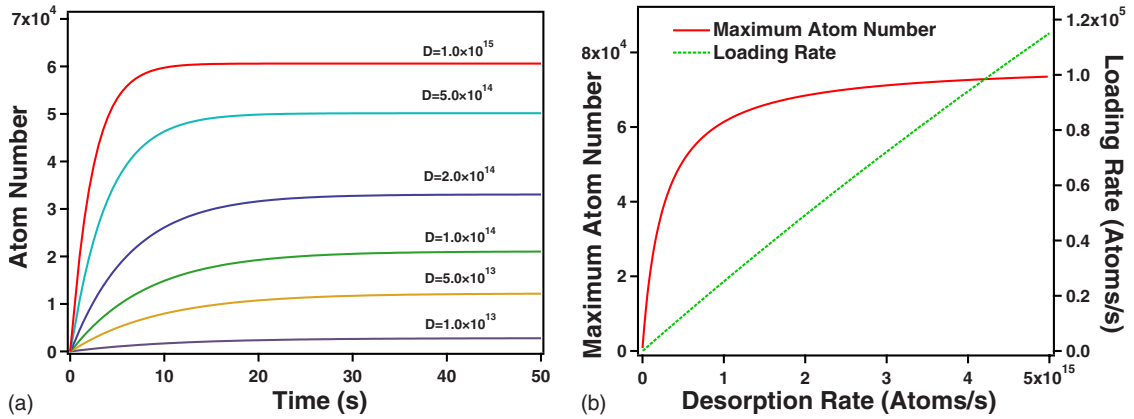

FIG. 2. (Color online) (a) Time evolution of the atom number with different desorption rates from 1.0×10^{13} to 5.0×10^{15} atoms/s. (b) The maximum atom number (solid red line) and the loading rate (dashed green line) versus the desorption rate D. The maximum atom number increases very quickly at the beginning when the desorption rate increases but it is saturating at the higher desorption rates. Parameters: $T=300$ K, $m=2.21\times10^{-25}$ kg, $V=1.35\times10^{-14}$ m^3, $\sigma=2\times10^{-17}$ m^2, $A=14$ s^{-1}, and $c=1/11.2$ s^{-1}.

$$N(t) = N_B + ae^{-(be^{-At}+Abt+Act)/A} \times \int_0^t e^{-A\tau+(be^{-A\tau}+Ab\tau+Ac\tau)/A}(e^{A\tau}-1)d\tau, \quad (8)$$

where N_B is the number of background atoms in the MOT with the blue LIAD light turned off.

Usually, the value of b/A is very small (see below for details), and we approximately have $\exp(-be^{-At}/A)\approx 1$, and Eq. (8) can be simplified to

$$N(t) = N_B + \frac{a}{b+c}[1-e^{-(b+c)t}]. \quad (9)$$

The steady-state atom number and the loading rate are given by

$$N_{ss} = N_B + \frac{a}{b+c} = N_B + \frac{0.5V^{2/3}v_c^4(m/2kT)^{3/2}\dfrac{D}{A}}{\sigma\sqrt{\dfrac{3kT}{m}}\dfrac{D}{A}+\dfrac{1}{\tau_b}}, \quad (10.1)$$

and

$$R \approx a = 0.5V^{2/3}v_c^4(m/2kT)^{3/2}\frac{D}{A}. \quad (10.2)$$

III. NUMERICAL RESULTS

According to expression (8) we could examine the time evolution of the atom number in the MOT as functions of the various experimental parameters, such as the desorption rate D, the adsorption coefficient A as well as the loss rate $c=1/\tau_b$ resulting from the background gas. The maximum number of atoms and the loading rate can also be scrutinized in detail. Let's look at the influences of the different parameters.

A. Desorption rate D

The desorption rate is the most important parameter to control the loading process in experiment. A previous experiment [12] based on Rb atoms has shown that a large atom number and high loading rate can be obtained either by increasing the intensity of the desorption light or by using the desorption light with shorter wavelength. Equation (8) reveals how the atom number in the MOT evolves quantitatively with different desorption rates D. Theoretical results based on our system are shown in Fig. 2(a). The corresponding parameters for our system include the temperature $T=300$ K, the mass of cesium atom $m=2.206\times10^{-25}$ kg, the trapping volume $V=1.35\times10^{-14}$ m^3, the capture velocity of the atoms $v_c\approx55$ m/s, the collision cross section of $\sigma=2\times10^{-17}$ m^2 and two parameters of the system $A=14.0$ s^{-1} and $c=1/11.2$ s^{-1}. (These two parameters can be obtained experimentally; see Sec. V.) We can see that the atom number increases at the beginning of the loading process and reaches equilibrium after several seconds. Higher desorption rates correspond to shorter times of reaching the saturated atom number.

According to the loading process of the MOT, the evolution of the maximum atom number (solid red line) and the loading rate (dashed green line) with desorption rates are shown in Fig. 2(b). It is clear that the maximum atom number increases very quickly at the beginning when the desorption rate increases but it saturates with high desorption rates. The reason is that the maximum atom number is limited by the specifics of the MOT, such as the trapping volume, the capture velocity of the atoms and so on, while the loading rate increases almost linearly with the desorption rates.

B. Adsorption coefficient A

The adsorption rate is another important parameter that affects the loading process of the MOT. Owing to the adsorption process, the background vacuum pressure can be restored very quickly when stopping the LIAD process. Figure 3(a) shows the time evolution of atom number versus the adsorption coefficient A. Here we have chosen $D=15.5\times10^{13}$ atoms/s and all the other parameters are the same as in Fig. 2. It is reasonable that lower adsorption coefficient implies a higher obtainable atom number, but this adsorption coefficient is determined by the material and con-

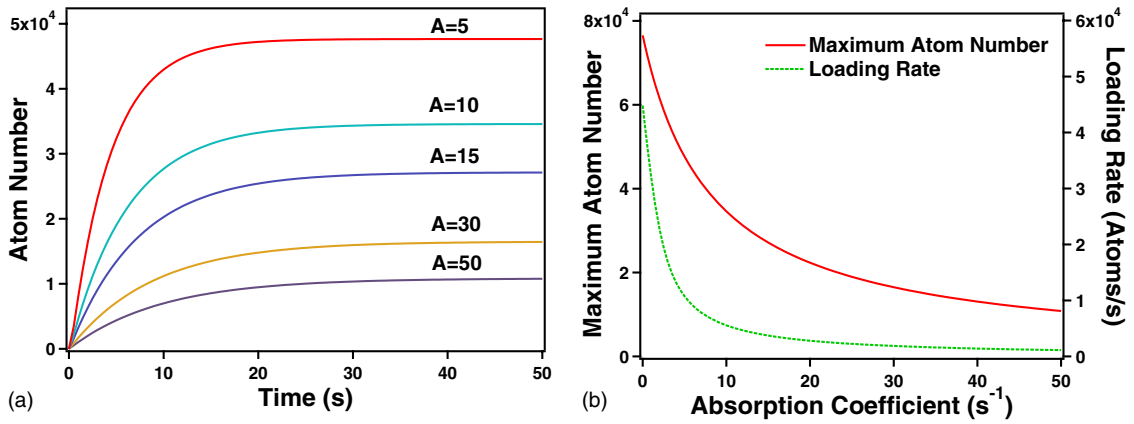

FIG. 3. (Color online) (a) Time evolution of the atom number versus various adsorption coefficient A. (b) The maximum atom number (solid red line) and the loading rate (dashed green line) versus the adsorption coefficient A. The large adsorption coefficient corresponds to the lower maximum atom number and lower loading rate. Here $D=15.5\times10^{13}$ atoms/s and all other parameters are the same as Fig. 2.

tents of the given vacuum system, which cannot be changed after the system has been set up. Experimentally, the background pressure can be reflected by the loading rate. In [12] the decay time of the loading rate after shutting off the desorption light was measured to be about 200 ms. This short restoration time is essentially determined by the adsorption rate $(1/A)$.

In Fig. 3(b) we show the maximum atom number (solid red line) and the loading rate (dashed green line) as a function of the adsorption coefficient. We can see that large adsorption coefficient (short decay time) corresponds to lower maximum atom number and lower loading rate. This may bring some troubles for those experiments needing large amount of atoms, such as the BEC experiments. But for manipulation of a few atoms or a single atom, it is acceptable. Higher adsorption coefficient means shorter restoration time, which is desirable, but if the adsorption coefficient is too big, the saturated atom number is small. Seeking a balance between the adsorption and the desorption is always an important issue in the experiment.

C. Loss rate ($c=1/\tau_b$) due to the background pressure

In the theoretical model we have considered the extra loss rate $(c=1/\tau_b)$ due to the background gas other than the cesium atoms. As we know, all cold atom experiments need a very good vacuum system. A bad vacuum pressure would dramatically increase the loss of atoms. Figure 4(a) shows the time evolution of the atom number as a function of the coefficient c (Here $D=15.5\times10^{13}$ atoms/s and $A=14$ s^{-1}). The results are summarized in Fig. 4(b), which shows that the loading rate (dashed green line) has almost no change with the increasing of loss rate from the background noncesium atoms, while the maximum atom number (solid red line) in the MOT is strongly affected by the background gas.

IV. EXPERIMENTAL SETUP

The real experimental system is shown in Fig. 5. The experiment is done in a transparent quartz cell with dimensions $30\times30\times125$ mm^3 and thickness of 5 mm. The cesium dispenser is positioned the back of the cell with a distance of about 70 mm from the MOT. An aspheric lens mounted on the oxygen-free copper is used to focus the dipole trap beam for optical microtrap of the single atoms. A microcavity formed by two supermirrors is glued on the copper bulk for the cavity QED experiment. The optical system for the MOT is quite conventional but designed for single

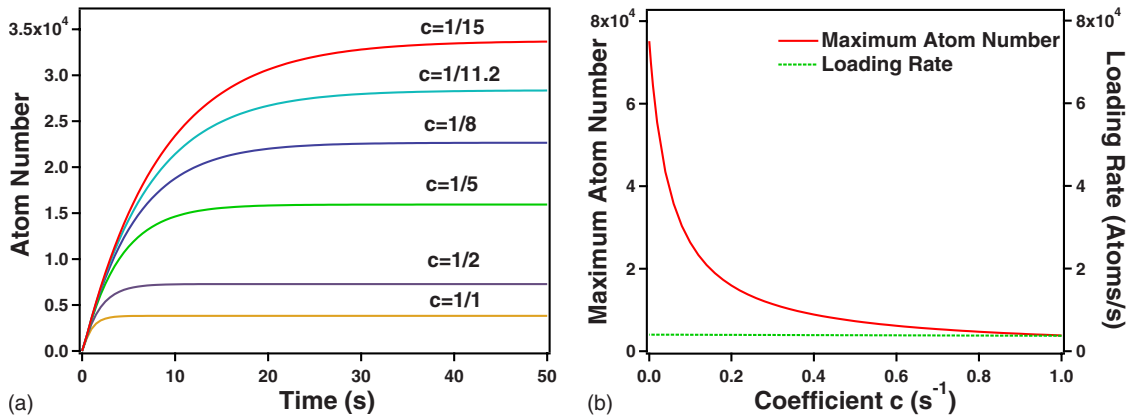

FIG. 4. (Color online) (a) Time evolution of the atom number versus the coefficient c. (b) The maximum atom number (solid red line) and the loading rate (dashed green line) versus the coefficient c. The loading rate has almost no change with the increasing of loss rate from the noncesium atoms in the background, while the maximum atom number in the MOT is strongly affected by the background gas. Here $D=15.5\times10^{13}$ atoms/s, $A=14$ s^{-1} and all the other parameters are the same as Fig. 2.

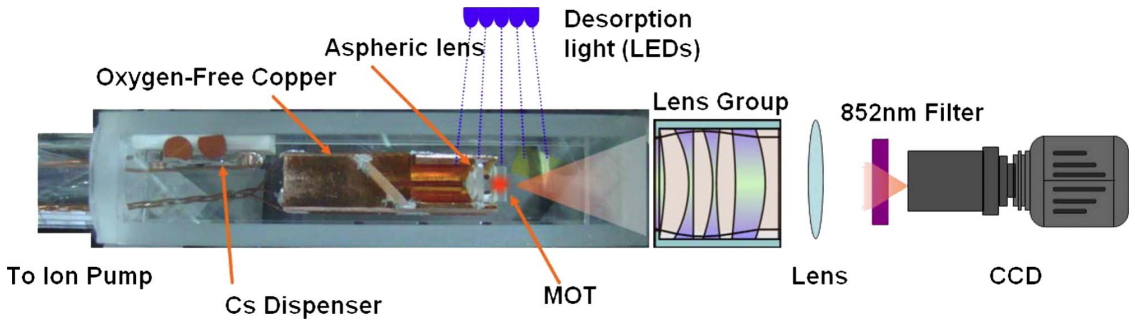

FIG. 5. (Color online) Experimental system. The MOT is performed in a transparent quartz cell. The cesium dispenser is positioned the back of the cell with a distance of about 70 mm from the MOT. The desorption light source made by seven bunched blue LEDs is located about 70 mm above the MOT. The fluorescence emitted from the cold atoms in the MOT is collected by a specially designed objective with numerical aperture NA=0.29 and is detected by a high-speed, low-noise CCD camera. There is a filter at center wavelength of 852 nm in front the CCD. An aspheric lens mounted on the oxygen-free copper is used to focus the dipole trap beam for optical microtrap of the single atoms. All of these are indicated in the figure.

atom manipulation. Two lasers provide the beams for cooling and repumping. The cooling beam is from an extended cavity diode laser (Toptica, DL-100), which is tuned 10.3 MHz below the transition of $6\ ^2S_{1/2}, F=4 \rightarrow 6\ ^2P_{3/2}, F'=5$ of cesium, and the total power is about 1.8 mW; The repumping beam is from a self-made diode laser, which is resonant to the transition of $6\ ^2S_{1/2}, F=3 \rightarrow 6\ ^2P_{3/2}, F'=4$, with total power of about 0.7 mW. The two beams are combined into a fiber and then split into three beams. The diameter of each beam is about 2 mm. The beams are circularly polarized with the retroreflected beams possessing the opposite circular polarization. The two coils provide a quadrupole magnetic field with the field gradient of about 22.5 G/cm. The desorption light source is made by seven bunched blue LEDs (central wavelength at 470 nm, LK-5BL, EK Japan Co. Ltd). The intensity of the irradiation can be changed by adjusting the driving current. These LEDs are located about 70 mm above the MOT. The fluorescence emitted from the cold atoms in the MOT is collected by a specially designed objective with numerical aperture NA=0.29. A high-speed, low-noise charge coupled device (CCD) camera (Princeton MicroMax 512BFT) is used to detect the fluorescence. The CCD camera with a filter at 852 nm is sensitive even to very small number of atoms in our experiment. The atom number can be inferred from the intensity of the fluorescence.

Before the desorption process we have heated the dispenser for about half an hour with an electrical current of 4A. The vacuum pressure is 7×10^{-9} Torr which is indicated by a vacuum gauge located about 28 cm away from the MOT. After the termination of the heating, the cell is left for two days and the equilibrium pressure is 3×10^{-10} Torr. The dispenser is switched off at all times during the following experimental measurements. It shows that the MOT can work well just by using the LIAD effect alone.

V. EXPERIMENTAL RESULTS AND DISCUSSIONS

A. MOT loading process

First we check the MOT loading process with different intensities of the desorption light. Figure 6 shows the time evolution of the atom number (colored solid triangles) measured by the CCD camera during the loading phase with various intensities of the blue light. The intensities increase from 0 to 1.76 mW/cm^2. Obviously the number of atoms loaded into the MOT can be changed effectively by varying the intensity of the blue light. The black solid lines in Fig. 6 are the theoretical fittings according to Eq. (8), which are good in agreement with the experimental results. From the fittings we have obtained the adsorption coefficient $A=(14.0 \pm 0.1)\ \mathrm{s}^{-1}$ and the loss rate caused by the noncesium atoms in the background is also determined as $c=(1/11.2 \pm 1/113.6)\ \mathrm{s}^{-1}$. For each intensity of blue light we obtain the corresponding desorption rates, which varies from $D=6.2 \times 10^{12}$ atoms/s to the maximum of 1.6×10^{14} atoms/s, which is limited by the present total intensity of blue light. The initial atom number N_B is about several hundreds of atoms, which is from the background gas.

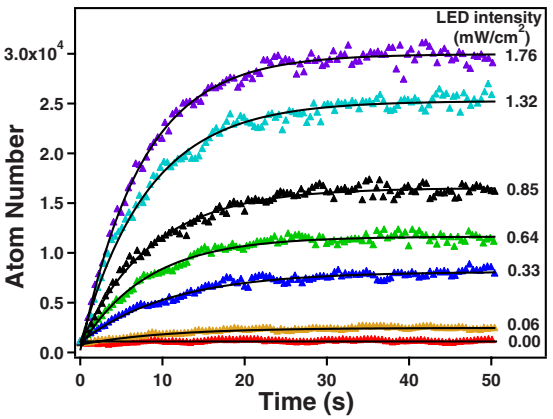

FIG. 6. (Color online) Time evolution of the atom number with different desorption intensity from 0 to 1.76 mW/cm^2. The colored solid triangles are the experimental data and the solid black lines are the theoretical fittings according to Eq. (8). The theoretical fittings are good in agreement with the experimental results. From the fittings we obtain the adsorption coefficient $A=(14.0 \pm 0.1)\ \mathrm{s}^{-1}$. The loss rate caused by the noncesium atoms in the background is also determined as $c=(1/11.2 \pm 1/113.6)\ \mathrm{s}^{-1}$. We also obtain the corresponding desorption rates, which varies from $D=6.2 \times 10^{12}$ atoms/s to the maximum of 1.6×10^{14} atoms/s for each intensity of blue light.

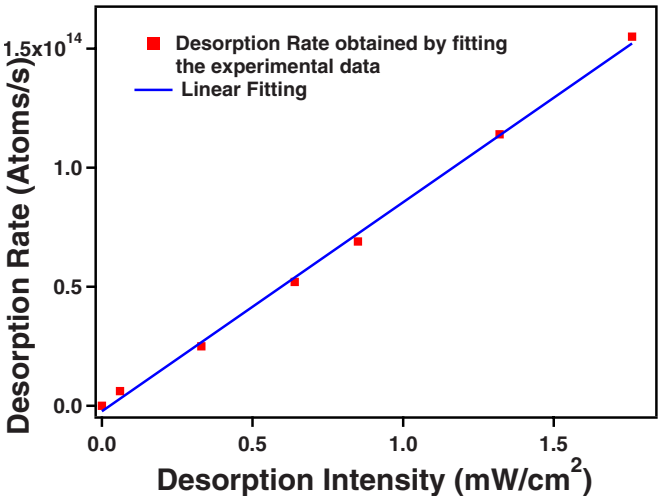

FIG. 7. (Color online) The desorption rate (red solid squares) versus the desorption intensity. The solid blue line is the linear fitting. The desorption rates increase linearly with the desorption light at relatively low intensities in our system.

The relationship between the desorption rates and the desorption blue light intensities is shown in Fig. 7. Clearly, the desorption rates (solid red squares) increase linearly with the desorption light at relatively low intensities in our system, while a saturated phase can be seen for sufficient intensity of the desorption light. The slope of the line is about 8.8×10^{13} atoms/(s mW/cm^2), which means that the increase in the atom number per second desorbed from the cell with every increased milliwatt per square centimeter of desorption intensity is 8.8×10^{13} atoms.

B. Maximum atom number and the loading rate

Figure 8(a) shows the maximum atom number versus the intensity of desorption light. The solid red squares are the experimental data while the solid green line is the theoretical fitting according to Eq. (8) with the obtained parameters: $A = 14.0$ s^{-1}, $c = 1/11.2$ s^{-1}. The theoretical fitting gives the prospective results when the desoption intensity increases to 50 mW/cm^2, though limited by the intensity of the present blue LEDs, what we have achieved is only 1.76 mW/cm^2. The inset in Fig. 8(a) shows a close up of the measured experimental points which are well fitted by Eq. (8). The potential maximum atom number with our system would reach more than 7×10^4 before it is saturated if we could further increase the intensity of the desorption light. For a maximum intensity of 1.76 mW/cm^2, we have achieved a maximum atom number of about 3.0×10^4.

As is shown in Fig. 2, the LIAD process can effectively increase the loading rates of the MOT. The corresponding experimental results (solid blue triangles) are shown in Fig. 8(b). The linear relationship is confirmed. For the maximum intensity of 1.76 mW/cm^2, we have achieved the maximum loading rate of about 4.0×10^3 atoms/s in the experiment. There is still room to obtain a higher loading rate if we could continue to increase the intensity of the blue light, but the rate of increase of the atom number is becoming small. Based on our experiment, we can increase the intensity of the blue light to about 10 mW/cm^2 to obtain maximum loading rate and get more atoms, while still keeping relatively good vacuum pressure for the long lifetime of the atom trap.

C. Adsorption coefficient *A*

The adsorption coefficient $A = 14.0 \pm 0.1$ s^{-1} for our system has been determined above. $1/A$ is about 70 ms which describes the decay time of the atom density in the cell after shutting off the desorption light. This parameter is very significant, as we have mentioned in Sec. II. The short decay time implies that the atom density and the vacuum pressure in the cell decay quickly to equilibrium. In other words the loading rate of the MOT decays to equilibrium in about 70 ms. This short restoration time essentially depends on the vacuum chamber as well as the adsorption coefficient. Better vacuum pressure and larger adsorption coefficient imply shorter decay time. We could not directly measure the decay

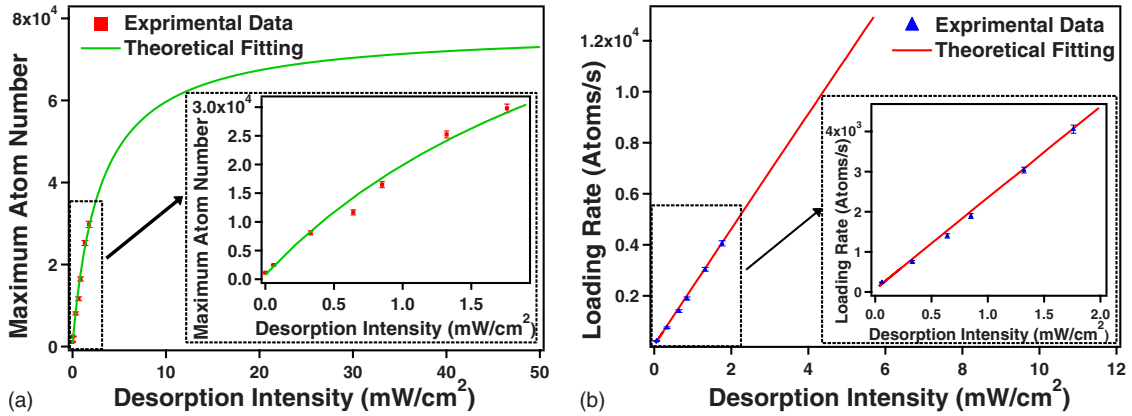

FIG. 8. (Color online) (a) Maximum atom number in the MOT versus the desorption intensity. The red solid squares are the experimental data while the solid green line is theoretical fitting according to Eq. (8). The inset shows the zoom of the experiment results and the fitting. The theoretical fittings are good in agreement with the experimental results with the obtained parameters: $A = 14.0$ s^{-1} and $c = 1/11.2$ s^{-1}. (b) The loading rates versus the desorption intensity. The blue solid triangles are the experimental data while the solid red line is the theoretical fitting according to Eq. (8). For the maximum intensity of 1.76 mW/cm^2, we have achieved the maximum loading rate of about 4.0×10^3 atoms/s in the experiment.

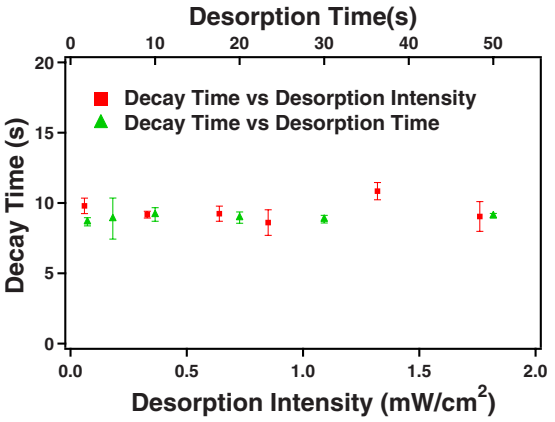

FIG. 9. (Color online) The decay time versus the desorption time (red solid squares) and the desorption intensity (green solid triangles). The decay time is obviously independent on the desorption time and the desorption intensity.

time constant of the Cs vapor pressure as was done by Klempt *et al.* [12] because the time scale was too short compared to the loading time constant of the MOT. Measurements performed by Klempt *et al.* were performed at a much higher Rb vapor pressure and gave a decay time for the background vapor pressure of 200 ms.

D. Decay time of atom number in the MOT after shutting off the desorption light and the background pressure

We have also measured the decay of atom number in the MOT after shutting off the desorption light using two different methods. In the first method we turn on the desorption light with an intensity of 1.32 $\mathrm{mW/cm^2}$ at the beginning while measuring the atom number when the desorption light shines for 2 to 50 s, then we shut the blue light off and measure the decays of the atom number in the MOT. In the second method we choose various desorption intensities from 0.06 to 1.76 $\mathrm{mW/cm^2}$ and for each round, the blue light shines for 50 s. The MOT approaches steady state and then we shut off the blue light to make the decay measurements. The results of all the measurements are shown in Fig. 9. It shows clearly that in both cases the decay times are about 9.2 s on average, which is independent of both the desorption time (solid green triangles) or the desorption intensity (solid red squares). The reason is that the vacuum system returns to equilibrium in only about 70 ms, as discussed above, and we could not see this transient process. The slow atom decay after the vacuum system reaches equilibrium is exponential and this is simply due to collisions between the cesium atoms in the MOT and the background atoms [32]. The background gases include the untrapped cesium atoms and the noncesium atoms. This decay time characterizes the vacuum pressure when the vacuum system reaches equilibrium.

Based on the loss rate caused by the noncesium atoms in the background, $c=1/\tau_b=(1/11.2\pm1/113.6)\ \mathrm{s^{-1}}$ and the measured total decay time (see Fig. 9) $1/\tau=(1/9.2\pm1/105.8)\ \mathrm{s^{-1}}$, we can obtain the partial pressures of the cesium atoms and the noncesium atoms. According to the relation: $1/\tau=1/\tau_{Cs}+1/\tau_b$, we obtain $1/\tau_{Cs}=(1/51.5\pm1/118.7)\ \mathrm{s^{-1}}$. So the partial pressure of noncesium atoms in the background is $(6.4\pm0.6)\times10^{-10}$ Torr and the pressure of untrapped cesium atoms in the background is $(1.4\pm0.2)\times10^{-10}$ Torr. The inferred pressure of the noncesium atoms is larger than the initial pressure we have measured before we start the experiment, 3×10^{-10} Torr. The reason is that the vacuum gauge is located about 28 cm away from the MOT and there is a pressure difference between them (see Fig. 5).

VI. CONCLUSIONS

In conclusion, we have theoretically and experimentally investigated the loading of cesium atom MOT only using the blue LIAD as the atom source. A simple model is used to simulate the adsorption and desorption process which can describe the experimental results very well. The relations between the maximum atom number, the loading rate and the desorption rate D, adsorption coefficient A, and the loss rate of the background c were established. The experiment was performed in an ultrahigh vacuum cell. It shows that, by using the commercial blue LEDs at center wavelength of about 470 nm, the loading rates and the number of cesium atoms in the MOT can be effectively controlled by varying either the time of the desorption or the intensity of the blue light, without the use of the dispenser or the secondary atom source. This LIAD system based on cesium atoms provides a convenient tool of manipulating atoms with long storage times of traps for further experiments.

The analysis of the loading process based on the atom rate equation is quite consistent with the experimental results. We eventually determine the parameters of system. The desorption rate D is about 1.55×10^{14} atoms/s for the blue light intensity of 1.76 $\mathrm{mW/cm^2}$. The adsorption coefficient A is about $(14.0\pm0.1)\ \mathrm{s^{-1}}$ and the loss rate of background c is about $(1/11.2\pm1/113.6)\ \mathrm{s^{-1}}$. We confirm that the vacuum pressure returns to equilibrium very quickly in about 70 ms after shutting off the blue light, which is not dependent on the process of LIAD, but only on the adsorption of the system. The partial pressures caused by noncesium atoms and the untrapped cesium atoms are all determined according to the partial pressure theorem.

ACKNOWLEDGMENTS

T.C.Z. would like to thank Daniel Comparat for useful discussions. We would like to acknowledge the support from the National Natural Science Foundation of China (Grants No. 60578018, No. 60808006, No. 60821004, No. 10974125, and No. 60978017), the 973 Program (Grant No. 2006CB921102), and the Natural Science Foundation of Shanxi (Grant No. 2008021003). This work is also supported partially by NCET project (Grant No. NCET-07-0524) and MXZX (Grant No. 08121019).

[1] H. J. Metcalf and P. van der Straten, *Laser Cooling and Trapping* (Springer, New York, 1999).
[2] E. L. Raab M. Prentiss, Alex Cable, Steven Chu, and D. E. Pritchard, Phys. Rev. Lett. **59**, 2631 (1987).
[3] A. L. Migdall, J. V. Prodan, W. D. Phillips, T. H. Bergeman, and H. J. Metcalf, Phys. Rev. Lett. **54**, 2596 (1985).
[4] J. D. Miller, R. A. Cline, and D. J. Heinzen, Phys. Rev. A **47**, R4567 (1993).
[5] S. Friebel, C. D'Andrea, J. Walz, M. Weitz, and T. W. Hansch, Phys. Rev. A **57**, R20 (1998).
[6] J. Ye, D. W. Vernooy, and H. J. Kimble, Phys. Rev. Lett. **83**, 4987 (1999).
[7] N. Schlosser, G. Reymond, I. Protsenko, and P. Grangier, Nature (London) **411**, 1024 (2001).
[8] J. Wang, J. Wang, S. Yan, T. Gen, and T. Zhang, Rev. Sci. Instrum. **79**, 123116 (2008).
[9] J. Fortagh, A. Grossman, T. W. Hänsch, and C. Zimmermann, J. Appl. Phys. **84**, 6499 (1998).
[10] A. Gozzini, F. Mango, J. H. Xu, G. Alzetta, F. Maccarone, and R. A. Bernheim, Nuovo Cimento D **15**, 709 (1993).
[11] E. Mariotti, S. Atutov, M. Meucci, P. Bicchi, C. Marinelli, and L. Moi, Chem. Phys. **187**, 111 (1994).
[12] C. Klempt, T. van Zoest, T. Henninger, O. Topic, E. Rasel, W. Ertmer, and J. Arlt, Phys. Rev. A **73**, 013410 (2006).
[13] J. H. Xu, A. Gozzini, F. Mango, G. Alzetta, and R. A. Bernheim, Phys. Rev. A **54**, 3146 (1996).
[14] A. M. Bonch-Bruevich, T. A. Vartanyan, S. G. Przhibel'skii, and V. V. Khromov, Phys. Usp. **41**, 834 (1998).
[15] S. N. Atutov, V. Biancalana, P. Bicchi, C. Marinelli, E. Mariotti, M. Meucci, A. Nagel, K. A. Nasyrov, S. Rachini, and L. Moi, Phys. Rev. A **60**, 4693 (1999).
[16] E. B. Alexandrov, M. V. Balabas, D. Budker, D. English, D. F. Kimball, C.-H. Li, and V. V. Yashchuk, Phys. Rev. A **66**, 042903 (2002).
[17] S. Gozzini and A. Lucchesini, Eur. Phys. J. D **28**, 157 (2004).
[18] J. Brewer and H. G. Rubahn, Chem. Phys. **303**, 1 (2004).
[19] A. Burchianti, C. Marinelli, A. Bogi, J. Brewer, K. Rubahn, H. G. Rubahn, F. Della Valle, E. Mariotti, V. Biancalana, S. Veronesi, and L. Moi, Europhys. Lett. **67**, 983 (2004).
[20] M. T. Graf, D. F. Kimball, S. M. Rochester, K. Kerner, C. Wong, D. Budker, E. B. Alexandrov, M. V. Balabas, and V. V. Yashchuk, Phys. Rev. A **72**, 023401 (2005).
[21] A. Burchianti, A. Bogi, C. Marinelli, C. Maibohm, E. Mariotti, and L. Moi, Phys. Rev. Lett. **97**, 157404 (2006).
[22] A. Cappello, C. de Mauro, A. Bogi, A. Burchianti, S. Di Renzone, A. Khanbekyan, C. Marinelli, E. Mariotti, L. Tomassetti, and L. Moi, J. Chem. Phys. **127**, 044706 (2007).
[23] A. Burchianti, A. Bogi, C. Marinelli, E. Mariotti, and L. Moi, Opt. Express **16**, 1377 (2008).
[24] T. Karaulanov, M. T. Graf, D. English, S. M. Rochester, Y. J. Rosen, K. Tsigutkin, D. Budker, E. B. Alexandrov, M. V. Balabas, D. F. Jackson Kimball, F. A. Narducci, S. Pustelny, and V. V. Yashchuk, Phys. Rev. A **79**, 012902 (2009).
[25] A. Hatakeyama, K. Oe, K. Ota, S. Hara, J. Arai, T. Yabuzaki, and A. R. Young, Phys. Rev. Lett. **84**, 1407 (2000).
[26] A. Hatakeyama, K. Enomoto, N. Sugimoto, and T. Yabuzaki, Phys. Rev. A **65**, 022904 (2002).
[27] A. Hatakeyama, K. Enomoto, and T. Yabuzaki, Phys. Scr., T **110**, 294 (2004).
[28] B. P. Anderson and M. A. Kasevich, Phys. Rev. A **63**, 023404 (2001).
[29] S. N. Atutov, R. Calabrese, V. Guidi, B. Mai, A. G. Rudavets, E. Scansani, L. Tomassetti, V. Biancalana, A. Burchianti, C. Marinelli, E. Mariotti, L. Moi, and S. Veronesi, Phys. Rev. A **67**, 053401 (2003).
[30] C. Monroe, W. Swann, H. Robinson, and C. Wieman, Phys. Rev. Lett. **65**, 1571 (1990).
[31] T. G. Walker and P. Feng, Adv. At., Mol., Opt. Phys. **34**, 125 (1994).
[32] S. Bali, K. M. O'Hara, M. E. Gehm, S. R. Granade, and J. E. Thomas, Phys. Rev. A **60**, R29 (1999).